AlN thin films grown on epitaxial 3C–SiC (100) for piezoelectric resonant devices

Chih-Ming Lin,[1,2,a)] Wei-Cheng Lien,[2] Valery V. Felmetsger,[3] Matthew A. Hopcroft,[2,4] Debbie G. Senesky,[1,2] and Albert P. Pisano[1,2]
[1]*Department of Mechanical Engineering, University of California, Berkeley, California 94720, USA*
[2]*Berkeley Sensor and Actuator Center, University of California, Berkeley, California 94720, USA*
[3]*OEM Group Incorporated, Gilbert, Arizona 85233, USA*
[4]*Hewlett-Packard Laboratories, Palo Alto, California 94304, USA*

(Received 17 August 2010; accepted 8 September 2010; published online 6 October 2010)

Highly *c*-axis oriented heteroepitaxial aluminum nitride (AlN) films were grown on epitaxial cubic silicon carbide (3C–SiC) layers on Si (100) substrates using alternating current reactive magnetron sputtering at temperatures between approximately 300–450 °C. The AlN films were characterized by x-ray diffraction, scanning electron microscope, and transmission electron microscopy. A two-port surface acoustic wave device was fabricated on the AlN/3C–SiC/Si composite structure, and an expected Rayleigh mode exhibited a high acoustic velocity of 5200 m/s. The results demonstrate the potential of utilizing AlN films on epitaxial 3C–SiC layers to create piezoelectric resonant devices. © *2010 American Institute of Physics*. [doi:10.1063/1.3495782]

Recently, AlN-based resonant devices have generated interest for wireless transmission systems. For example, piezoelectric AlN thin films have been used to fabricate a variety of radio frequency (RF) resonators and filters, such as layered surface acoustic wave (SAW) devices,[1,2] thin film bulk acoustic resonators,[3] contour mode resonators,[4] and Lamb wave resonators.[5,6] These devices are enabled by the high acoustic velocity, high electromechanical coupling coefficient, and chemical inertness of AlN thin films. However, due to limitations in material properties, AlN-based resonators have some natural drawbacks, such as a lower quality factor (Q) in comparison to quartz-based resonators.

The use of low mechanical loss materials such as single crystal silicon (Si), sapphire (Al_2O_3), quartz (SiO_2), and silicon carbide (SiC) as substrates can decrease the mechanical loss and increase the Q of piezoelectric resonant devices.[7] Although SiO_2 (Ref. 8) and Si (Refs. 9 and 10) have been reported to efficiently enhance the Q of piezoelectric resonators, the low acoustic velocities of SiO_2 and Si are disadvantage for high-frequency devices. In contrast, SiC has a high acoustic velocity up to 13 000 m/s. Therefore, SiC warrants the investigation of enhancing the Q of AlN-based resonant devices without compromising the resonance frequency.

It is well reported that, although SiC has over 200 different crystal symmetries, the cubic (3C–SiC) and hexagonal (4H–SiC and 6H–SiC) polytypes are most commonly synthesized.[11] Recently, several research groups have investigated and demonstrated the deposition of AlN thin films onto 4H–SiC (Ref. 12) and 6H–SiC (Ref. 13) substrates. However, AlN thin films grown on hexagonal SiC polytypes are unsuitable for fabrication of piezoelectric resonant devices because the growth of epitaxial 4H–SiC and 6H–SiC thin films is currently limited to SiC substrates of the same polytypes.[11] To date, only the growth of epitaxial 3C–SiC films on Si substrates have been demonstrated. The use of Si substrates is advantageous as Si is low-cost and various Si bulk micromachining techniques are well-established.

In this study, highly *c*-axis oriented AlN thin films grown on epitaxial 3C–SiC layers on Si (100) substrates using alternating current (ac) reactive magnetron sputtering are developed and experimentally characterized. Although AlN (0002) and 3C–SiC (100) film have a lattice mismatch of 28.6 %, this challenge was addressed by a two-step deposition process. AlN films deposited on epitaxial 3C–SiC layers were characterized using the x-ray diffraction (XRD) (Siemens D5000), scanning electron microscope (SEM) (Leo 1550), and transmission electron microscopy (TEM) (Jeol 2100F).

For this research, commercially available wafers (NOVASiC Inc.) with 2.3-μm-thick epitaxial 3C–SiC layers grown on Si (100) were used as the substrates. AlN thin films with various thicknesses in the range of 0.5–3 μm were deposited on 3C–SiC/Si (100) substrates by ac (40 kHz) powered S-Gun magnetron.[14] Prior to AlN film deposition, the surface of the epitaxial 3C–SiC layer was treated by low energy (150–200 eV) Ar ions from capacitively coupled RF (13.56 MHz) plasma. To mitigate the effect of the lattice mismatch between AlN (0002) and 3C–SiC (100), a 50-nm-thick AlN seed layer was deposited with high nitrogen (N_2) concentration in argon (Ar) and N_2 gas mixture. These initial grains served as the seeds for the growth of higher quality columnar grains as the AlN film thickness increased. This seed layer also served to reduce the negative effect of lattice mismatch between AlN (0002) and 3C–SiC (100).

The deposition processes were performed at the ambient temperature (300–350 °C) for the majority of the AlN film thickness but at an elevated temperature (approximately 450 °C), using an external infrared heater, for the 50-nm-thick AlN seed layer. The S-Gun magnetron was powered with an ac power of 3 kW during the seed layer deposition and 5.5 kW during the deposition of the remaining AlN film, providing a deposition rate of 66 nm/min. The detailed process recipes are listed as following steps:

(1) RF plasma etching at RF power=200 W and Ar flow=5 SCCM (SCCM denotes cubic centimeter per minute at STP) for 600 s.

a)Author to whom correspondence should be addressed. Electronic mail: gimmylin@berkeley.edu.

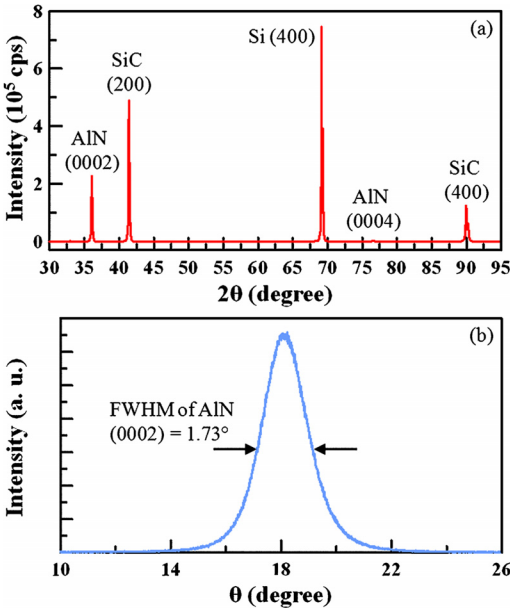

FIG. 1. (Color online) (a) XRD spectrum of the AlN(0002)/3C–SiC(100)/Si(100) layered structure where the AlN film is 1 μm and the 3C–SiC layer is 2.3 μm. (b) Rocking curve of 1-μm-thick AlN (0002) film deposited on the epitaxial 3C–SiC layer on the Si (100) substrate.

(2) Wafer preheat for 50 s (maximum temperature is about 350 °C).
(3) 50-nm-thick AlN seed layer deposition at the elevated temperature (approximately 450 °C), ac power =3 kW, Ar flow=4 SCCM, and N_2 flow =25 SCCM.
(4) AlN layer deposition at the ambient temperature (300–350 °C), ac power=5.5 kW, Ar flow =6 SCCM, and N_2 flow=17 SCCM.

The crystalline structure was determined by XRD as shown in Fig. 1(a) where the diffraction peaks correspond to a hexagonal wurtzite-type AlN (0002) film, a cubic zinc-blende-type SiC (100) film, and a Si (100) substrate, respectively. The presence of (0002) and (0004) AlN reflections at 36.07° and 76.46°, respectively, give the indication of a highly *c*-axis oriented AlN thin film that has been grown on the epitaxial 3C–SiC (100) layer. As shown in Fig. 1(b), the rocking curve of the 1-μm-thick AlN film shows a full width at half maximum (FWHM) value of 1.73° which implies the AlN film has good crystallinity.

Deposition at the ambient temperature or elevated temperature was employed to investigate the effect on AlN crystallinity as shown in Fig. 2. The rocking curve FWHM of the AlN film was reduced from 2.61 to 2.29° when the seed layer deposition temperature was raised from the ambient temperature (300–350 °C) to the elevated temperature (approximately 450 °C). In fact, sustained heating at the elevated temperature during the entire deposition process did not markedly improve the crystal orientation, indicating that higher adatom mobility is required mostly at the nucleation stage where it allows the grain formation with fewer structural defects and releases the lattice mismatch of AlN (0002) and 3C–SiC (100) as well.

In addition to the sputtering temperatures, the degree of *c*-axis texturing of the reactively sputtered AlN film is closely related to the substrate texture and the surface roughness. The surface pretreatment of the epitaxial 3C–SiC layer

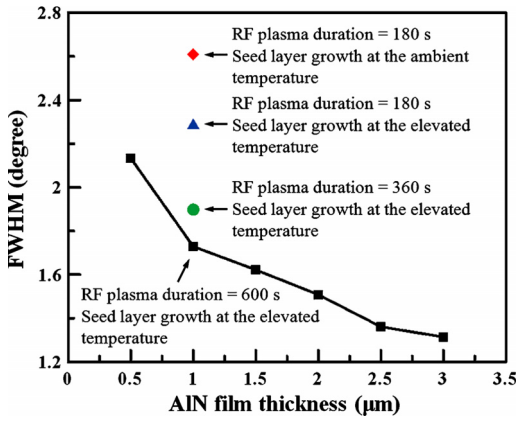

FIG. 2. (Color online) Plot of the measured FWHM of AlN thin films grown under different deposition conditions vs AlN film thicknesses.

can significantly influence the AlN film orientation. It is well-known that predeposition RF plasma etching can improve the film nucleation and coalescence processes due to removal of impurities. Furthermore, the RF plasma etching can decrease the surface roughness of the 3C–SiC layer and hence can improve the AlN crystal alignment. As depicted in Fig. 2, 1-μm-thick AlN films with different RF plasma etching duration of 180 s, 360 s, and 600 s exhibit the FWHM values of 2.29°, 1.89°, and 1.73°, respectively. As a result, the longer RF plasma etching duration of 600 s is required to achieve the best crystallinity of AlN films on the epitaxial 3C–SiC (100) layer. For comparison, the RF plasma etching duration of 180 s is enough to achieve highly *c*-axis oriented AlN films on Si substrates under the same sputter conditions. This phenomenon might be due to the higher atomic binding energy and the lower sputtering yield of SiC. The sputtering yield ratio for SiC to Si is approximately 0.5.[15]

The cross-sectional SEM image of the AlN/3C–SiC/Si composite structure is shown in Fig. 3(a) where the AlN and 3C–SiC film thicknesses are 1 μm and 2.3 μm, respectively. The void defects with trapezoid shape at the 3C–SiC/Si interface are due to silicon outdiffusion.[16] As shown in Fig. 3(b), the AlN seed layer and textured AlN layer can be identified in the bright field (BF) TEM image. It is clear that the AlN thin film exhibits numerous columnar grains which are perpendicular to the surface of the epitaxial 3C–SiC layer. Figure 3(c) shows a typical high resolution (HR) TEM image of the interface between the AlN and 3C–SiC layers. The HRTEM image reveals an amorphous AlN starting layer between AlN and 3C–SiC layers which has been previously reported to appear at the beginning of AlN sputtering processes.[17] The electron diffraction (ED) patterns of 1-μm-thick AlN (0002) film and 2.3-μm-thick epitaxial 3C–SiC (100) film along the [110] zone axis are shown in Figs. 3(d) and 3(e), respectively. This result supports the conclusion that the AlN grains on the epitaxial 3C–SiC layer are well-textured and approximately along the same direction.

In order to demonstrate the practical operation of piezoelectric AlN films grown on epitaxial 3C–SiC (100) layers, a two-port SAW device was fabricated on the AlN/3C–SiC/Si composite structure in which surface acoustic waves propagate in the plane normal to the *c*-axis of AlN film and along the [011] direction of 3C–SiC/Si (100) substrate. The design parameters of the SAW device are summarized and listed in Table I. The transmission characteristics of the SAW device were measured using an Agilent E5071B network analyzer.

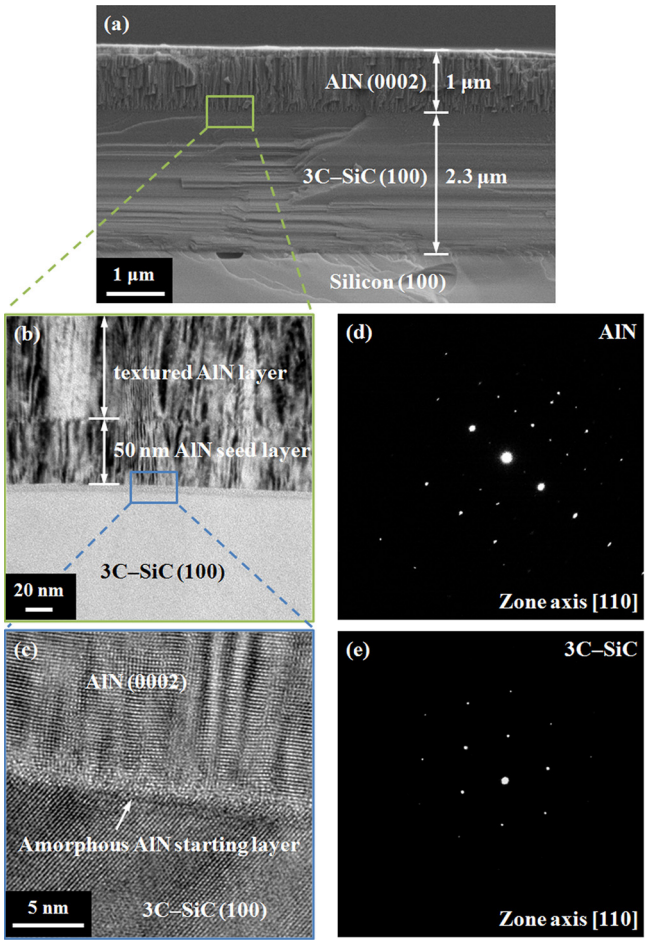

FIG. 3. (Color online) (a) Cross-sectional SEM image of 1-μm-thick AlN (0002) film on the epitaxial 3C–SiC layer on the Si (100) substrate. (b) Cross-sectional BF TEM image of the interface between AlN (0002) and 3C–SiC (100). (c) Cross-sectional HRTEM image of the interface between AlN (0002) and 3C–SiC (100). An amorphous AlN starting layer appeared at the beginning of AlN sputtering process. (d) ED pattern of 1-μm-thick AlN (0002) film grown on the epitaxial 3C–SiC (100) layer along the [110] zone axis of AlN. (e) ED pattern of 2.3-μm-thick epitaxial 3C–SiC layer grown on the Si (100) substrate along the [110] zone axis of 3C–SiC.

Figure 4 details the measured frequency response of the SAW device after time-gating which was employed to remove the feedthrough effect. An expected Rayleigh mode exhibited a center frequency of 260 MHz as well as a high acoustic velocity up to 5200 m/s for the 1-μm-thick AlN film and the 2.3-μm-thick epitaxial 3C–SiC film on the Si substrate. This result confirms that the AlN/3C–SiC/Si structure possesses a high acoustic velocity which enables high-frequency SAW devices.[18]

Highly *c*-axis oriented AlN thin films were deposited on epitaxial 3C–SiC layers on Si (100) substrates using ac reactive magnetron sputtering. A two-step deposition process was used to overcome the lattice mismatch of 28.6 % between AlN (0002) and 3C–SiC (100). The lowest FWHM value of 1.31° was achieved with a 3-μm-thick AlN film grown on the epitaxial 3C–SiC (100) layer. A two-port SAW device on the AlN/3C–SiC/Si composite structure exhibited the Rayleigh mode with an acoustic velocity of 5200 m/s. The results confirm that the AlN thin films on the epitaxial 3C–SiC (100) layers can be utilized to create high-frequency piezoelectric resonant devices.

TABLE I. Design parameters of the SAW device.

Number of interdigital transducer (IDT) pairs	40
Aperture (μm)	400
IDT electrode width (μm)	5
Metallization ratio	0.5
Delay line (μm)	400
Al electrode thickness (nm)	150

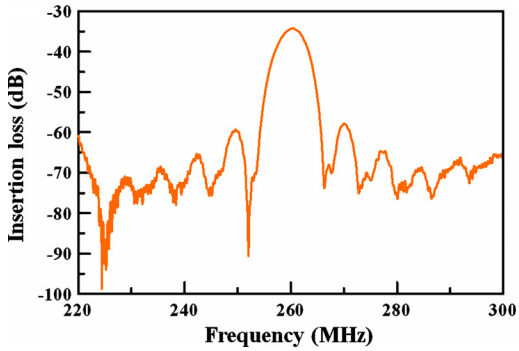

FIG. 4. (Color online) Measured frequency responses of the SAW device on the AlN/3C–SiC/Si layered structure after time-gating.

This work was supported by the DARPA Chip-Scale Mechanical Spectrum Analyzers (CSSA) award (Grant No. NGC-8140000613) under the DARPA Microsystems Technology Office (MTO).

[1] L. G. Pearce, R. L. Gunshor, and R. F. Pierret, Appl. Phys. Lett. **39**, 878 (1981).
[2] C.-M. Lin, Y.-Y. Chen, and T.-T. Wu, J. Phys. D: Appl. Phys. **39**, 466 (2006).
[3] J. S. Wang and K. M. Lakin, Appl. Phys. Lett. **40**, 308 (1982).
[4] G. Piazza, P. J. Stephanou, and A. P. Pisano, J. Microelectromech. Syst. **15**, 1406 (2006).
[5] J. Bjurström, I. Katardjiev, and V. Yantchev, Appl. Phys. Lett. **86**, 154103 (2005).
[6] C.-M. Lin, T.-T. Yen, Y.-J. Lai, V. V. Felmetsger, M. A. Hopcroft, J. H. Kuypers, and A. P. Pisano, IEEE Trans. Ultrason. Ferroelectr. Freq. Control **57**, 524 (2010).
[7] F. S. Hickernell, Proceedings of IEEE International Ultrasonics Symposium, 1998, p. 273.
[8] A. Artieda and P. Muralt, IEEE Trans. Ultrason. Ferroelectr. Freq. Control **55**, 2463 (2008).
[9] R. Abdolvand, H. M. Lavasani, G. K. Ho, and F. Ayazi, IEEE Trans. Ultrason. Ferroelectr. Freq. Control **55**, 2596 (2008).
[10] H. Chandrahalim, S. A. Bhave, R. Polcawich, J. Pulskamp, D. Judy, R. Kaul, and M. Dubey, Appl. Phys. Lett. **93**, 233504 (2008).
[11] M. Mehregany, C. A. Zorman, S. Roy, A. J. Fleischman, C.-H. Wu, and N. Rajan, Int. Mater. Rev. **45**, 85 (2000).
[12] Y. Takagaki, P. V. Santos, E. Wiebicke, O. Brandt, H.-P. Schonherr, and K. H. Ploog, Appl. Phys. Lett. **81**, 2538 (2002).
[13] K. Uehara, C.-M. Yang, T. Furusho, S.-K. Kim, S. Kameda, H. Nakase, S. Nishino, and K. Tsubouchi, Proceedings of IEEE International Ultrasonics Symposium, 2003, p. 905.
[14] V. V. Felmetsger, P. N. Laptev, and S. M. Tanner, J. Vac. Sci. Technol. A **27**, 417 (2009).
[15] V. Cimalla, J. Pezoldt, and O. Ambacher, J. Phys. D: Appl. Phys. **40**, 6386 (2007).
[16] W.-C. Lien, N. Ferralis, C. Carraro, and R. Maboudian, Cryst. Growth Des. **10**, 36 (2010).
[17] R. Aigner, Proceedings of 3rd International Symposium of Acoustic Wave Devices for Future Mobile Communication Systems, Chiba, Japan, 2007, p. 85.
[18] Y.-Y. Chen, T.-T. Wu, and T.-T. Chou, J. Phys. D: Appl. Phys. **37**, 120 (2004).